PHYSICAL REVIEW E **88**, 010101(R) (2013)

Single-particle tracking data reveal anticorrelated fractional Brownian motion in crowded fluids

Matthias Weiss*

Experimental Physics I, University of Bayreuth, Universitätsstrasse 30, D-95440 Bayreuth, Germany

(Received 24 April 2013; revised manuscript received 14 June 2013; published 8 July 2013)

Anomalous diffusion with a sublinear growth of the particles' mean-square displacement (subdiffusion) has been observed frequently in crowded fluids, e.g., in the cytoplasm of living cells or in artificial solutions. Based on a recently reported set of single-particle tracking data, it is shown here that trajectories of nanoparticles immersed in artificial crowded fluids display all signatures of anticorrelated fractional Brownian motion. Moreover, the trajectories' power spectrum follows a scaling that reports on the fluid's viscoelasticity. Macromolecular crowding therefore renders fluids viscoelastic which in turn leads to subdiffusion of immersed tracer particles with all the characteristics of fractional Brownian motion.

DOI: 10.1103/PhysRevE.88.010101 PACS number(s): 05.40.Fb, 02.50.Ey, 87.15.Vv

Many intracellular fluids are crowded with a plethora of macromolecules with a total concentration of up to 400 mg/ml [1]. Due to crowding, changes in (bio)chemical reactions are anticipated (see [2] for a recent review). A striking example for altered biochemical reactions is the phosphorylation pattern of the mitogen-activated protein kinase (MAPK) that has been shown to vary strongly with the degree of cytoplasmic crowding [3]. Besides excluded volume effects that constrain the available reaction space, also an altered diffusion of macromolecules has been invoked to explain these results [4]. Indeed, diffusion is known to be slowed down by macromolecular crowding [5], and diffusion also has been frequently reported to display an anomalous characteristics (see [6] for a recent comprehensive review). In particular, the mean-square displacement (MSD) of diffusing particles has been shown to grow for several orders of magnitude as $\langle r_\tau^2 \rangle \sim \tau^\alpha$ with $\alpha < 1$ ("subdiffusion"). For time and length scales beyond a few seconds and a few micrometers, normal diffusion as an asymptotic mode of motion is restored (see, e.g., discussion in [7,8]).

To rationalize the emergence of subdiffusion in unconfined crowded fluids, several random-walk models have been proposed. The most popular ones are obstructed diffusion (OD), i.e., the motion of a tracer particle in a fractal, percolation-like network of obstacles [9]; fractional Brownian motion (FBM) with anticorrelated diffusion steps [10]; and a continuous time random walk (CTRW) in which diffusing tracers take power-law distributed rests between periods of free diffusion [11,12]. While a decision in favor of one of these models for subdiffusion in the cytoplasm of living cells is still pending, we have recently reported strong evidence that FBM is the mode of motion of nanometer-sized beads in artificial crowded solutions [8]: Based on a cycling orbit strategy [13,14], particles were tracked in concentrated sucrose or dextran solutions over many minutes with a temporal resolution of 4 ms and a spatial accuracy of about 10 nm. While beads showed normal diffusion in sucrose solutions, a subdiffusive behavior $\langle r_\tau^2 \rangle \sim \tau^\alpha$ with $\alpha \approx 0.8$ was observed for dextran solutions on time scales below ~5 s. An evaluation of the extraordinary long single-particle tracking data ($>10^5$ positions per trajectory) in terms of the random walk's asphericity revealed that the beads' motion in dextran solutions was most consistent with FBM. Simulation results for OD or (truncated) CTRW models were inconsistent with the experimentally found asphericity values. This indicated that FBM is the best description for particle trajectories in dextran solutions. Yet, using the asphericity to distinguish different types of random walks is, like other recent approaches [15], a rather indirect approach. If sufficient statistics are available in the recorded trajectories, key features of individual random-walk models, e.g., an anticorrelation of successive steps, can be probed directly.

Here we revisit the single-particle tracking data reported in Ref. [8] to probe whether the observed subdiffusion in dextran solutions shows the major hallmarks of FBM: Gaussian statistics of displacements (or increments) and an anticorrelation in successive random steps. The latter is the major reason for the emergence of subdiffusion in FBM as it reflects a memory in the particle's random walk. In particular, it will be shown below that trajectories in sucrose and dextran solutions indeed show stationary Gaussian statistics of increments. In addition, trajectories in dextran solutions show a pronounced anticorrelation of successive steps that is not seen for diffusion in sucrose solutions. Subdiffusion in crowded dextran solutions therefore has all the signatures of fractional Brownian motion. Moreover, the power spectra of trajectories in dextran solutions show a nontrivial scaling $S(\omega) \sim 1/\omega^{1+\alpha}$ that reports on the viscoelastic character of the fluid.

For the analysis, previously published data from a single-particle orbit tracking approach on nanometer-sized beads are used [8]. Particles have been tracked over extended time scales in concentrated sucrose and dextran solutions with a time resolution of $\Delta t = 4$ ms. Each of the two-dimensional trajectories considered for the analysis below contained more than 10^5 positions. For experimental details the reader is referred to [8].

To probe whether the recorded trajectories have a stationary Gaussian distribution of increments, the cumulative distribution of squared displacements $P(r_\tau^2)$ for different time lags $\tau = k\Delta t$ ($k = 1,2,\ldots$) is considered. In contrast to a probability distribution function (PDF), the cumulative distribution has the advantage of not requiring any binning of the data into a histogram. Using the cumulative distribution function has been very beneficial when investigating diffusion in two dimensions [16,17]. In brief, a Gaussian PDF of increments in two

*matthias.weiss@uni-bayreuth.de

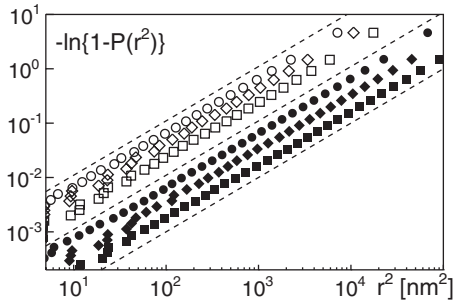

FIG. 1. Representative examples of the cumulative distribution of squared displacements [Eq. (1)] for sucrose and dextran solutions (full and open symbols, respectively). Data are shown as $-\ln[1-P(r_\tau^2)]$ vs r_τ^2 in double-logarithmic style. A linear scaling (dashed lines) is anticipated for random walks with a Gaussian PDF of increments. All data sets follow this scaling over several orders of magnitude ($\tau = 0.1, 0.4, 1.6$ s shown as circles, diamonds, and squares, respectively).

dimensions is given by $p(r)r\,dr = 2\exp(-r^2/\sigma^2)/\sigma^2 r\,dr$. Changing variables to squared displacements ($\xi = r^2$) and integrating the PDF yields the cumulative distribution function of squared increments:

$$P(r_\tau^2) = \int_0^{r_\tau^2} e^{-\xi/\sigma^2}/\sigma^2 d\xi = 1 - e^{-r_\tau^2/\sigma^2}\ . \qquad (1)$$

If the PDF of increments of the recorded random walk is Gaussian, then plotting the cumulative distribution function as $-\ln[1-P(r_\tau^2)]$ vs r_τ^2 should result in a linear function with the slope reporting on the mean-square displacement, $\sigma^2 = \langle r_\tau^2\rangle$. Deviations from a linear relation therefore are a clear signature for a non-Gaussian statistics of increments.

As can be seen in Fig. 1, trajectories in sucrose and dextran solutions show indeed a linear relation $-\ln[1-P(r_\tau^2)] \sim r_\tau^2$ for various lag times τ. This result confirms the hypothesis that trajectories in both solutions have a stationary Gaussian distribution of increments. In addition, the mean-square displacement σ^2 derived from $P(r_\tau^2)$ follows the previously reported scaling [8] $\langle r_\tau^2\rangle \sim \tau^\alpha$ for sucrose ($\alpha \approx 1$) and dextran ($\alpha \approx 0.8$) solutions (Fig. 2, inset). For dextran solutions, a crossover to normal diffusion for lag times beyond $\tau \sim 1$s is also visible. This confirms the long-lasting yet nonasymptotic nature of the observed subdiffusion in crowded fluids. Please note that the results on the time-averaged MSD (Fig. 2, inset) have been reported already in [8].

Rescaling the squared displacements with the respective MSD ($x = r_\tau^2/\langle r_\tau^2\rangle$) leads to a collapse of all cumulative distributions onto a single master curve of the form $P(x) = 1 - \exp(-x)$ (see Fig. 2). This demonstrates that all trajectories are governed by Gaussian statistics of diffusion increments irrespective of the lag time τ and the considered fluid.

A potential (anti)correlation of successive displacements in the trajectories, as predicted by FBM, can be probed by the average scalar product of normalized successive increment vectors,

$$C_\tau(t) = \left\langle \frac{\mathbf{v}_\tau(T)}{|\mathbf{v}_\tau(T)|} \cdot \frac{\mathbf{v}_\tau(t+T)}{|\mathbf{v}_\tau(t+T)|} \right\rangle_T , \qquad (2)$$

with the increment vectors $\mathbf{v}_\tau(t) = \mathbf{r}(t+\tau) - \mathbf{r}(t)$. Similar correlation functions have been used already to characterize

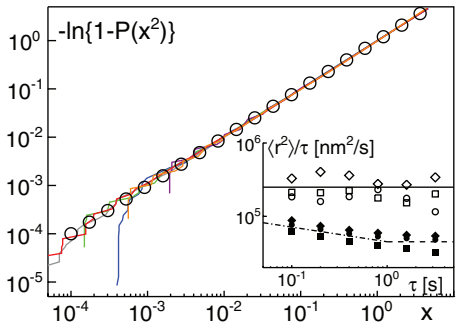

FIG. 2. (Color online) Rescaling the squared increments of Fig. 1 with their respective MSD, $x = r_\tau^2/\langle r_\tau^2\rangle$, leads to a collapse of all data (colored lines) to a single, parameter-free master curve $P(x) = 1 - e^{-x}$, i.e., all data follow the prediction $-\ln[1-P(x)] = x$ over several orders of magnitude (indicated by open circles). Thus, all trajectories have a Gaussian PDF of increments irrespective of the lag time τ. Inset: The MSD used for rescaling shows the previously reported subdiffusion [8]. For sucrose solutions (open symbols), $\langle r_\tau^2\rangle/\tau = \text{const}$ (full line); for dextran solutions (closed symbols) $\langle r_\tau^2\rangle/\tau \sim 1/\tau^{0.2}$ (dash-dotted line). Beyond $\tau \sim 1$ s, data for dextran solutions converge towards normal diffusion (dashed line). Data for dextran solutions have been shifted up by a factor 5 for better visibility.

trajectories of (anomalous) random walks [18,19]. For a Markovian random walk, i.e., normal diffusion, this quantity is expected to decay from unity (at $t = 0$) to zero for $t = \tau$. In contrast, FBM should show a significant anticorrelation, i.e., $C_\tau < 0$ for $t \approx \tau$. Simulations of normal diffusion and FBM (see [8] for details on simulating FBM) confirm this expectation (Fig. 3, insets). In line with this prediction, data for sucrose showed a rapid decay towards zero for all tested values of τ [Fig. 3(a)]. The beads' random walk therefore shows no memory and is hence a Markovian random walk. In contrast, data for dextran solutions show a significant anticorrelation ($C_\tau < 0$) in the range $0 < t < \tau$ for several τ, in agreement with the predictions of FBM [Fig. 3(b)]. While an asymptotic version of FBM (which shows subdiffusion on all time scales) should exhibit the same negative value of C_τ for all τ [Fig. 3(b), inset], our experimental data indicate a convergence $\min(C_\tau) \to 0$ that reflects again the crossover towards normal Brownian motion for large time scales τ. Thus, trajectories in crowded dextran solutions show indeed on intermediate time scales the hallmark of FBM, namely, anticorrelated displacements.

To confirm that dextran solutions feature FBM and not OD, the number of distinct sites s_τ visited within a period τ was determined. A recent report [15] predicted a scaling $s_\tau/\langle r_\tau^2\rangle \sim \tau^\delta$ with $\delta = 0$ for FBM with $\alpha \leqslant 1$, and $\delta < 0$ for OD. Indeed, data for sucrose and dextran solutions agree with the prediction $\delta = 0$ for normal diffusion and FBM, respectively (Fig. 4).

Apart from the type of (sub)diffusion, trajectories of single-particle tracking experiments can also be used to determine material properties of the surrounding fluid. The Fourier-transformed trajectory, for example, yields information about the complex shear modulus $G(\omega) = G'(\omega) + iG''(\omega)$ of the fluid [20]. Elastic contributions are summarized in $G'(\omega)$ whereas viscous effects are reflected in $G''(\omega)$. Hence, $G(\omega) \approx G'(\omega)$ for rubber and $G(\omega) \approx iG''(\omega)$ for liquid water. Viscoelastic fluids have real and imaginary parts of similar

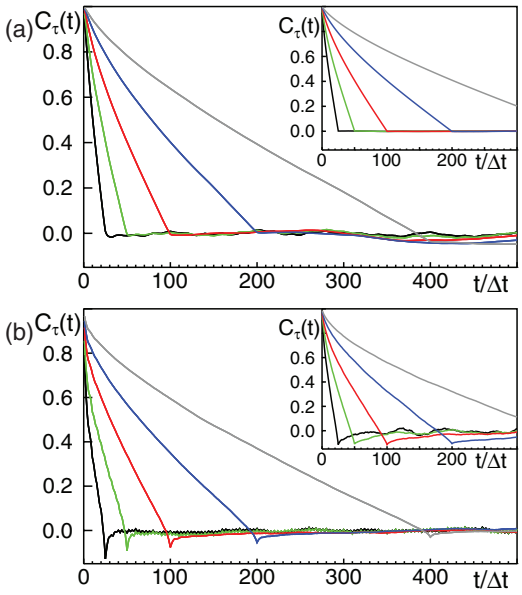

FIG. 3. (Color online) (a) The correlation function of particle displacements, $C_\tau(t)$ [Eq. (2)], shows a rapid decay from unity towards zero in sucrose solutions, in agreement with simulation results on normal Brownian motion (inset). Colored lines represent time lags $\tau = 0.1, 0.2, 0.4, 0.8, 1.6$ s (shown left to right, respectively, as black, green, red, blue, and grey). (b) In contrast, data for dextran solutions show a pronounced anticorrelation [$C_\tau(t) < 0$] after an initial correlation decay towards zero. This result is in favorable agreement with simulation data on FBM (inset), therefore confirming that trajectories in dextran solutions have all the features of an anticorrelated FBM. Here, $\Delta t = 4$ ms is the trajectories' temporal resolution.

magnitude. Moreover, viscoelastic fluids are characterized by a scaling $|G(\omega)| \sim \omega^\alpha$ which is also reflected in the power spectrum of single-particle trajectories in these environments: $S(\omega) \sim 1/\omega^{1+\alpha}$. For purely viscous fluids, normal Brownian motion is anticipated, and a scaling $S(\omega) \sim 1/\omega^2$ is predicted. Indeed, our trajectories in sucrose solutions follow this prediction over several orders of magnitude [see example in Fig. 5(a)]. In contrast, the power spectrum of trajectories in crowded dextran fluids show a scaling $S(\omega) \sim 1/\omega^{1+\alpha}$ with $0.7 \leqslant \alpha \leqslant 0.9$ for high frequencies while the trivial scaling $S(\omega) \sim 1/\omega^2$ is seen for low frequencies. This corresponds

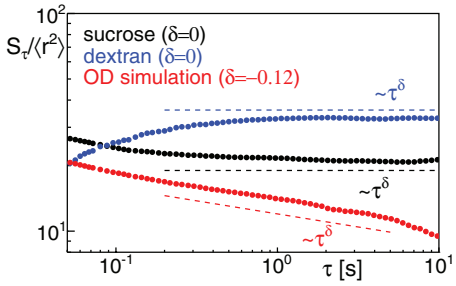

FIG. 4. (Color online) The number of distinct sites visited within a period τ divided by the MSD (averaged over three trajectories) shows a scaling $s_\tau/\langle r_\tau^2\rangle \sim \tau^\delta$ with $\delta = 0$ for both sets of experimental data, hence confirming FBM in dextran solutions. In contrast, simulations of OD show $\delta < 0$ as expected [15].

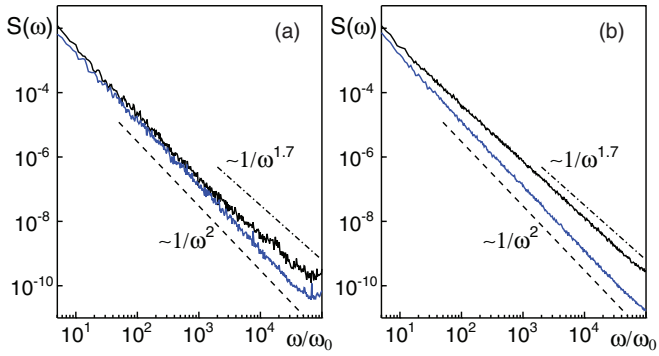

FIG. 5. (Color online) (a) The power spectrum $S(\omega)$ (averaged over three individual trajectories) in sucrose (blue) agrees well with the prediction for purely viscous fluids, $S(\omega) \sim 1/\omega^2$ (dashed line). In contrast, data for dextran solutions show a clear indication for fractional Gaussian noise and viscoelasticity in the high-frequency regime [dash-dotted line; $S(\omega) \sim 1/\omega^{1.7}$]. For better visibility, ω has been normalized by the smallest possible frequency ω_0, and $S(\omega_0)$ has been set to unity. (b) The power spectrum of simulated CTRW trajectories (blue) follow the scaling of a normal random walk, whereas obstructed diffusion at the percolation threshold (black) also yields a nontrivial scaling $S(\omega) \sim 1/\omega^{1.7}$.

nicely to our observation of subdiffusion on small time scales (high frequencies) and an asymptotic convergence towards normal diffusion for large times (low frequencies). Hence, sucrose solutions are purely viscous fluids whereas dextran solutions appear viscoelastic on certain frequency scales.

Interestingly, simulated trajectories for CTRW ($\alpha = 0.7$) and obstructed diffusion at the percolation threshold ($\alpha \approx 0.7$) show a scaling $S(\omega) \sim 1/\omega^2$ and $S(\omega) \sim 1/\omega^{1.7}$, respectively [Fig. 5(b)]. Simulations were performed as described previously [8]. This numerical result reveals that the scaling of $S(\omega)$ is sufficient to distinguish CTRW from FBM and obstructed diffusion. The latter two, however, have a similar nontrivial scaling of the power spectrum. Identifying FBM as the mode of motion as compared to OD therefore requires knowledge about the correlation of successive steps (see above). Moreover, arguing in favor of viscoelastic characteristics of a fluid on the basis of $S(\omega)$ may be an oversimplification since obstructed diffusion of tracers in (static) fractal structures yields the same scaling.

One may wonder why dextran-crowded fluids and sucrose solutions induce such different diffusion characteristics of tracer particles. While a full understanding of the phenomenon is not yet at hand, the following points may yield a basic rationale. Hard spheres with a mere excluded volume interaction do not show subdiffusion with a power law in the MSD over extended time scales. Hence, tracer particles that have similar sizes as solvent molecules (e.g., organic dyes in water) should not show subdiffusion. Large tracers in fluids with small solutes (e.g., sucrose) will experience a multitude of kicks from solvent and solute molecules that can be summarized again as a Markovian random impact, hence leading to normal diffusion with a certain diffusion constant. Yet, if crowders have similar sizes as the trace particle and also have, for example, internal degrees of freedom, a nontrivial behavior in the MSD may emerge. To this end, one may consider a tracer particle trying to move in a semidilute solution of

polymers (e.g., dextran). If the tracer performs a diffusive step, neighboring polymers will get squeezed which induces an elastic restoring force (polymers acting as entropic springs). This yields an anticorrelation of successive diffusion steps as anticipated in FBM. On larger time scales, the polymers will also move and a Markovian random walk of the tracer (and the neighboring crowders) is observed. This example may be taken as a simplified realization of FBM, linking the diffusion of tracer particles and the crowded fluid's viscoelasticity.

In summary, crowding renders dextran fluids viscoelastic on certain frequency scales which enforces subdiffusion of nanoparticles on corresponding time scales. As a consequence, the particles' random walk has all the features of FBM, namely, Gaussian statistics of increments and anticorrelated displacements.

Financial support by the Human Frontier Science Programme is gratefully acknowledged.

[1] J. Ellis and A. Minton, Nature **425**, 27 (2003).
[2] H. Zhou, G. Rivas, and A. Minton, Ann. Rev. Biophys. **37**, 375 (2008).
[3] K. Aoki, M. Yamada, K. Kunida, S. Yasuda, and M. Matsuda, Proc. Natl. Acad. Sci. USA **108**, 12675 (2011).
[4] M. Hellmann, D. Heermann, and M. Weiss, Europhys. Lett. **97**, 58004 (2012).
[5] J. Dix and A. Verkman, Ann. Rev. Biophys. **37**, 247 (2008).
[6] F. Höfling and T. Franosch, Rep. Prog. Phys. **76**, 046602 (2013).
[7] G. Guigas, C. Kalla, and M. Weiss, Biophys. J. **93**, 316 (2007).
[8] D. Ernst, M. Hellmann, J. Köhler, and M. Weiss, Soft Matter **8**, 4886 (2012).
[9] M. Saxton, Biophys. J. **66**, 394 (1994).
[10] J. Szymanski and M. Weiss, Phys. Rev. Lett. **103**, 038102 (2009).
[11] Y. He, S. Burov, R. Metzler, and E. Barkai, Phys. Rev. Lett. **101**, 058101 (2008).
[12] A. Lubelski, I. M. Sokolov, and J. Klafter, Phys. Rev. Lett. **100**, 250602 (2008).
[13] K. Kis-Petikova and E. Gratton, Microsc. Res. Tech. **63**, 34 (2004).
[14] Y. Katayama, O. Burkacky, M. Meyer, C. Brauchle, E. Gratton, and D. Lamb, ChemPhysChem **10**, 2458 (2009).
[15] Y. Meroz, I. M. Sokolov, and J. Klafter, Phys. Rev. Lett. **110**, 090601 (2013).
[16] J. Schutz, H. Schindler, and T. Schmidt, Biophys. J. **73**, 1073 (1997).
[17] G. Guigas and M. Weiss, Biophys. J. **91**, 2393 (2006).
[18] J. H. Jeon *et al.*, Phys. Rev. Lett. **106**, 048103 (2011).
[19] S. Burov, J. H. Jeon, R. Metzler, and E. Barkai, Phys. Chem. Chem. Phys. **13**, 1800 (2011).
[20] B. Schnurr, F. Gittes, F. MacKintosh, and C. Schmidt, Macromolecules **30**, 7781 (1997).